ADVANCED MATERIALS
www.advmat.de

Interfacial Superconductivity on the Topological Semimetal Tungsten Carbide Induced by Metal Deposition

Wenliang Zhu, Xingyuan Hou, Jing Li, Yifei Huang, Shuai Zhang, Junbao He, Dong Chen, Yiyan Wang, Qingxin Dong, Mengdi Zhang, Huaixin Yang, Zhian Ren, Jiangping Hu, Lei Shan, and Genfu Chen**

Interfaces between materials with different electronic ground states have become powerful platforms for creating and controlling novel quantum states of matter, in which inversion symmetry breaking and other effects at the interface may introduce additional electronic states. Among the emergent phenomena, superconductivity is of particular interest. Here, by depositing metal films on a newly identified topological semimetal tungsten carbide (WC) single crystal, interfacial superconductivity is obtained, evidenced from soft point-contact spectroscopy. This very robust phenomenon is demonstrated for a wide range of metal/WC interfaces, involving both nonmagnetic and ferromagnetic films, and the superconducting transition temperatures are surprisingly insensitive to the magnetism of thin films. This method offers an opportunity to explore the long-sought topological superconductivity and has potential applications in topological-state-based spin devices.

Searching for topological superconductors is a crucial step to find the expected new particles of Majorana fermions, and to generate Majorana zero modes, which can be used as a qubit for fault-tolerant quantum computation.[1–4] Generally, there are two routes to realize topological superconductivity. One scheme is to build artificial topological superconductors based on hybrid structures, for example, utilizing the proximity effect between an s-wave superconductor and a spin-nondegenerate metal.[5–8] The other scheme is to find intrinsic topological superconductors with spin-triplet odd-parity pairing. However, such a superconducting state has been very rare in nature with only very limited possible candidates.[9] A possible way to obtain intrinsic topological superconductors is to dope carriers into a topological insulator or topological semimetal.[10–12] Although there have been some instructive attempts in doped topological insulators,[13–16] the synthesis of superconducting samples with a particular doping level is difficult.[17] Furthermore, it is not easy to preserve the bulk band structures of the topological insulator after doping and to ensure the emergence of unconventional superconductivity prevailing over the conventional one.[16] On the other hand, some encouraging experiments have shown proximity-induced superconductivity on the surface of 3D topological insulators,[18,19] whereas their topological nature is yet to be confirmed. Recently, superconductivity has been observed at the point contacts formed between normal metal tips and some non-superconducting topological semimetals.[20–23] Most recently, tip-induced superconductivity was observed on tungsten carbide (WC), which is a new type of topological semimetal with super hardness.[24] Though the underline mechanism including local pressure, confinement effect and some kind of interface coupling between tip and sample was still not confirmed, yet these findings suggest a new way to explore topological superconductivity in a heterostructure based on two completely non-superconducting metals.

In this work, we show that the interfacial superconductivity possesses ubiquitously on the interface between WC single crystals and various metallic thin films. We deposited various metallic thin films on WC single crystals and performed conductance measurements on the films using soft point-contact technique. Andreev reflection signal was observed in the point-contact spectra for both nonmagnetic Au and Pt films and ferromagnetic Fe, Co, Ni films, supporting the existence of interfacial superconductivity. The compatibility of

W. Zhu, Dr. X. Hou, Dr. J. Li, Y. Huang, Dr. S. Zhang, Dr. J. He, Dr. D. Chen, Dr. Y. Wang, Q. Dong, M. Zhang, Prof. H. Yang, Prof. Z. Ren, Prof. J. Hu, Prof. L. Shan, Prof. G. Chen
Beijing National Laboratory for Condensed Matter Physics
Institute of Physics
Chinese Academy of Sciences
Beijing 100190, China
E-mail: lshan@iphy.ac.cn; gfchen@iphy.ac.cn

W. Zhu, Dr. J. Li, Y. Huang, Q. Dong, M. Zhang, Prof. H. Yang, Prof. Z. Ren, Prof. J. Hu, Prof. L. Shan, Prof. G. Chen
School of Physical Sciences
University of Chinese Academy of Sciences
Beijing 100190, China

Prof. H. Yang, Prof. Z. Ren, Prof. J. Hu, Prof. G. Chen
Songshan Lake Materials Laboratory
Dongguan, Guangdong 523808, China

Prof. L. Shan
Key Laboratory of Structure and Functional Regulation of Hybrid Materials of Ministry of Education
Institutes of Physical Science and Information Technology
Anhui University
Hefei 230601, China

The ORCID identification number(s) for the author(s) of this article can be found under https://doi.org/10.1002/adma.201907970.

DOI: 10.1002/adma.201907970

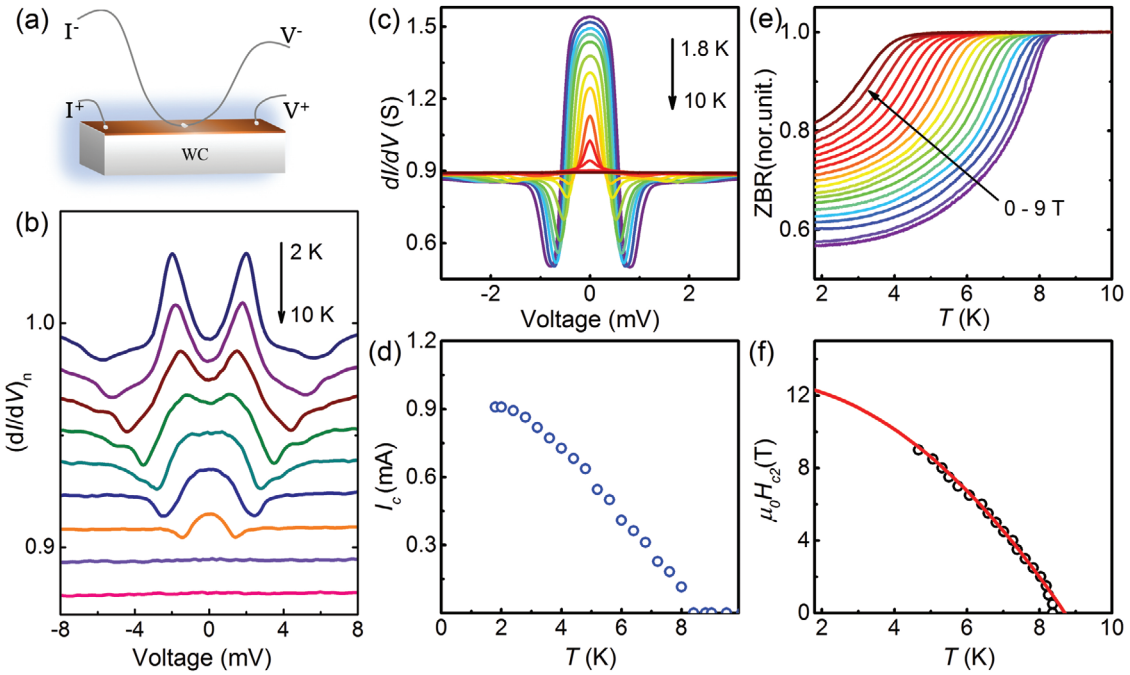

Figure 1. Evidence of superconductivity for nonmagnetic-film-coated WC single crystal detected by soft point-contact spectra. a) Schematic diagram showing the soft point-contact on the coating surface of WC sample and the differential conductance measurement electrodes. b) Temperature dependence of the normalized spectra in the intermediate regime for point-contact on Pt-coated WC, showing Andreev reflection peaks and dips due to critical current effect. c) Another representative point-contact spectra obtained on Au-coated WC in the thermal limit, showing a zero bias conductance peak (ZBCP) along with two dips. d) Temperature dependence of critical current I_c obtained from (c). e) Magnetic field dependence of point-contact zero bias resistance (ZBR) showing the suppression of superconducting transition. f) The $\mu_0 H_{c2}$–T_c phase diagram extracted from (e). Each critical temperature was determined by the derivation point of the ZBR curves. The red curve is a fit to the data using the empirical formula $\mu_0 H_{c2}(T) = \mu_0 H_{c2}(0)[1 - (T/T_c)^2]$.

the induced superconductivity with ferromagnetism reveals abnormal properties compared with the conventional superconductors. Thus, this study might open an avenue to realize topological superconductivity in a very simple way, and have great potential application in topological superconducting devices.

Figure 1a illustrates the geometry of our experiments. High-quality single crystals of WC were grown from Co-fluxes and metallic thin films were deposited on the WC surfaces by means of magnetron sputtering method with Au, Pt, Fe, Co, Ni targets, respectively. In general, interfacial superconductivity could only bear a very small critical current and an even smaller current has to be applied to detect such superconductivity. However, in our case, the current flows in a bulk crystal with very low resistance, the measured voltage will fall into the resolution limit of the nano-voltmeter before the interface becomes superconducting. Alternatively, the so-called "soft" point-contact technique was adopted here to examine the existence of superconductivity. The contact was made between a small drop (about 30–50 μm in diameter) of Ag paste and the coated WC surface and differential dI/dV–V spectra were measured by the standard lock-in technique. A real contact is usually composed of multiple parallel micro-constrictions/channels, and the size of some channels could be comparable to or even smaller than the mean free path of the sample,[25] which can be estimated as several micrometers from the transport experiments[26] (see Supporting Information).

Figure 1b shows a set of temperature-dependent point-contact spectra (dI/dV–V) measured on a Pt-coated WC. The temperature evolution of the spectral shape is in good agreement with that of the Andreev reflection spectra of a normal metal/superconductor (N/S) point contact. In the framework of Blonder–Tinkham–Klapwijk theory,[27–30] the symmetrical double peaks accompanied by a zero bias dip indicate a finite barrier at the N/S interface. Increase of barrier height will enhance the peaks and further depress the zero-bias conductance simultaneously. Another feature of the spectra in Figure 1b is two conductance dips located outside the Andreev reflection peaks. This usually originates from the critical current effect[31] that happens if the ballistic condition of $a \ll l$ cannot be well satisfied, where a is the contact radius and l is the electron mean free path. These features indicate that some channels in this contact locate in the intermediate regime. In the thermal regime of $a \gg l$, the critical current effect will dominate the spectral shape and lead to a zero-bias conductance peak (ZBCP) with two dips outside it,[32] as exemplified in Figure 1c. It can be seen that, with increasing temperature, the ZBCP decays continuously and finally fades away. Thus, by plotting zero-bias resistance (ZBR), the reciprocal of ZBCP as a function of temperature, we could obtain the superconducting transition and hence the transition onset temperature T_c, which is defined by the inflexion point in the R–T curves. Figure 1d shows the temperature dependence of critical current I_c derived from the observed dips. With the temperature decreasing, the critical current increases and then

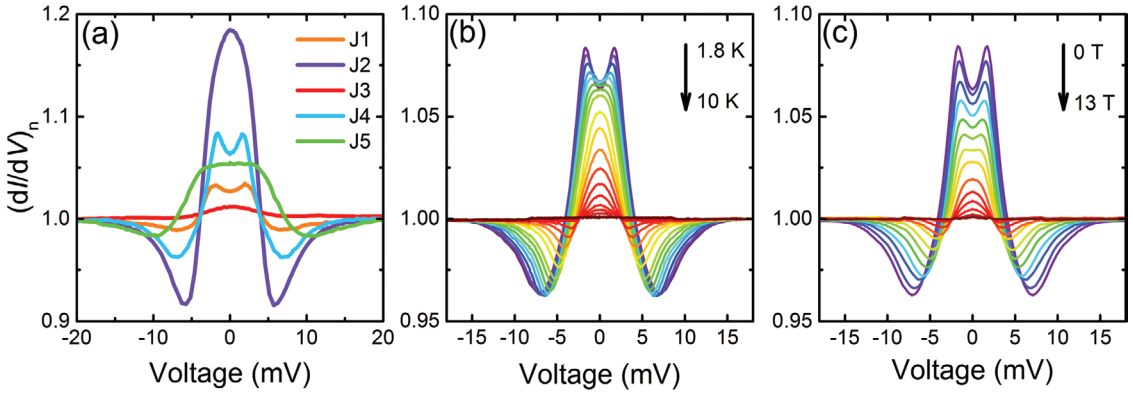

Figure 2. d*I*/d*V* spectra for magnetic Co-coated WC. a) Andreev reflection dominated and critical current effect dominated point-contact spectra acquired on different junctions on one sample coated by Co film. b) Temperature dependence of the normalized spectra in the intermediate regime for the junction J_3 in (a), showing Andreev reflection peaks and dips due to critical current effect. c) Field dependence of the normalized spectra in (b).

appears to be temperature independent at lower temperatures. This characteristic is similar to that of the interfacial superconductivity previously reported in $SrTiO_3/LaAlO_3$ system[33] and that of the superconducting Cd_3As_2 film.[34] The critical current was determined to be about 0.9 milliampere. Figure 1e presents a series of ZBR–*T* curves measured at different magnetic fields. The superconducting transition shifts towards lower temperatures with increasing fields, from which we could determine the critical magnetic field of $\mu_0 H_{c2}(T)$ as shown in Figure 1f with a zero-field transition temperature $T_c \approx 8.5$ K. The obtained $\mu_0 H_{c2}(T)$ can be described by the well-known empirical formula of $\mu_0 H_{c2}(T) = \mu_0 H_{c2}(0)[1 - (T/T_c)^2]$, which is usually appropriated for type-II superconductors.

The observation of superconductivity in such a hybrid structure is surprising by considering that it is built from a normal metal and WC which is not superconducting even under a high pressure up to 11 GPa.[35] We have tried to make soft point contact directly on the pristine WC single crystals but cannot see any obvious superconducting signals. The two findings exclude the tip induced pressure or confinement effect as the dominant reason of such interfacial superconductivity. Since the magnetron sputtering could build a better interface coupling than a soft contact, we thought that the coupling between normal metals and WC should be a key ingredient for the induced superconductivity. The thin metal layer has two possible roles. One is carrier doping into WC, leading to a sufficiently high density of states beneficial to superconductivity. The other one is dislocation-induced high density of states in heterostructures, giving rise to the interfacial superconductivity as proposed by Fu. et al.[36] At the present time, the microscopic details of the interfaces and the mechanism of interfacial coupling are still open questions. Further experimental and theoretical efforts are thus strongly desired to get a comprehensive understanding of this issue. As aforementioned, at low temperatures, the resistance drops rapidly below the resolution of voltmeter if we apply a small current using a standard four-point probe setup. On the contrary, a resistance drop up to 72% could be observed using a pseudo-four-point probe configuration (see Supporting Information). This allows us to explore the interfacial superconductivity without introducing any kind of damages or local strains. Since the point contact is a micro-region probe, we could examine the spatial extension of superconductivity by preparing lots of point contacts at random locations on the sample surface. More than 100 soft point contacts, usually 5 contacts on a single sample, have been studied and superconducting signal has been detected at almost all these point contacts (see Supporting Information and refer to **Figure 2**a), demonstrating that this is not a local effect.

In our previous experiments of hard point contact by means of needle–anvil method, tip-induced superconductivity has been realized on WC using both nonmagnetic and ferromagnetic tips.[24] So it made a lot of sense to explore superconductivity at the interface between WC and a ferromagnetic thin film. Figure 2a shows the spectra taken at five point contacts prepared on the same Co-coated WC single crystal. Either Andreev reflection signal or critical current effect can be seen in all the curves, indicating a wide extension of interfacial superconductivity. As shown in Figure 2b,c, temperature and magnetic field dependencies of the Andreev reflection spectra were measured in detail for a selected point contact. It can be seen that superconductivity is suppressed gradually with both temperature and field, similar to the Au-coated WC. Point-contact spectra have been measured for Fe-, Co-, and Ni-coated WC and the results are presented in **Figure 3**a–c, respectively. The corresponding superconducting transitions at magnetic fields are shown in Figure 3d–f, and the determined $\mu_0 H_{c2}(T)$s are given in Figure 3g–i. It is interesting to note that the $\mu_0 H_{c2}(T)$ relations can also be described by the above mentioned empirical formula. The good consistency among the data obtained from different metal films demonstrates that the observed resistance transitions may be of the same superconducting origin.

To get further insight into the interfacial superconductivity, we performed a large number of point-contact measurements by varying the thickness of metal layers. Since the sample surface is usually not that smooth, the thickness of the metal layer was acquired from the simultaneously deposited film on a Si substrate (see Supporting Information). We found that Co is more beneficial to induce the interface superconductivity than Pt, Au, Ni, and Fe and that the optimal thickness of Co layer is around 22 nm for high-performance superconductivity, but the critical temperature shows no obvious dependence on the coating thickness. When the thickness is beyond ≈60 nm,

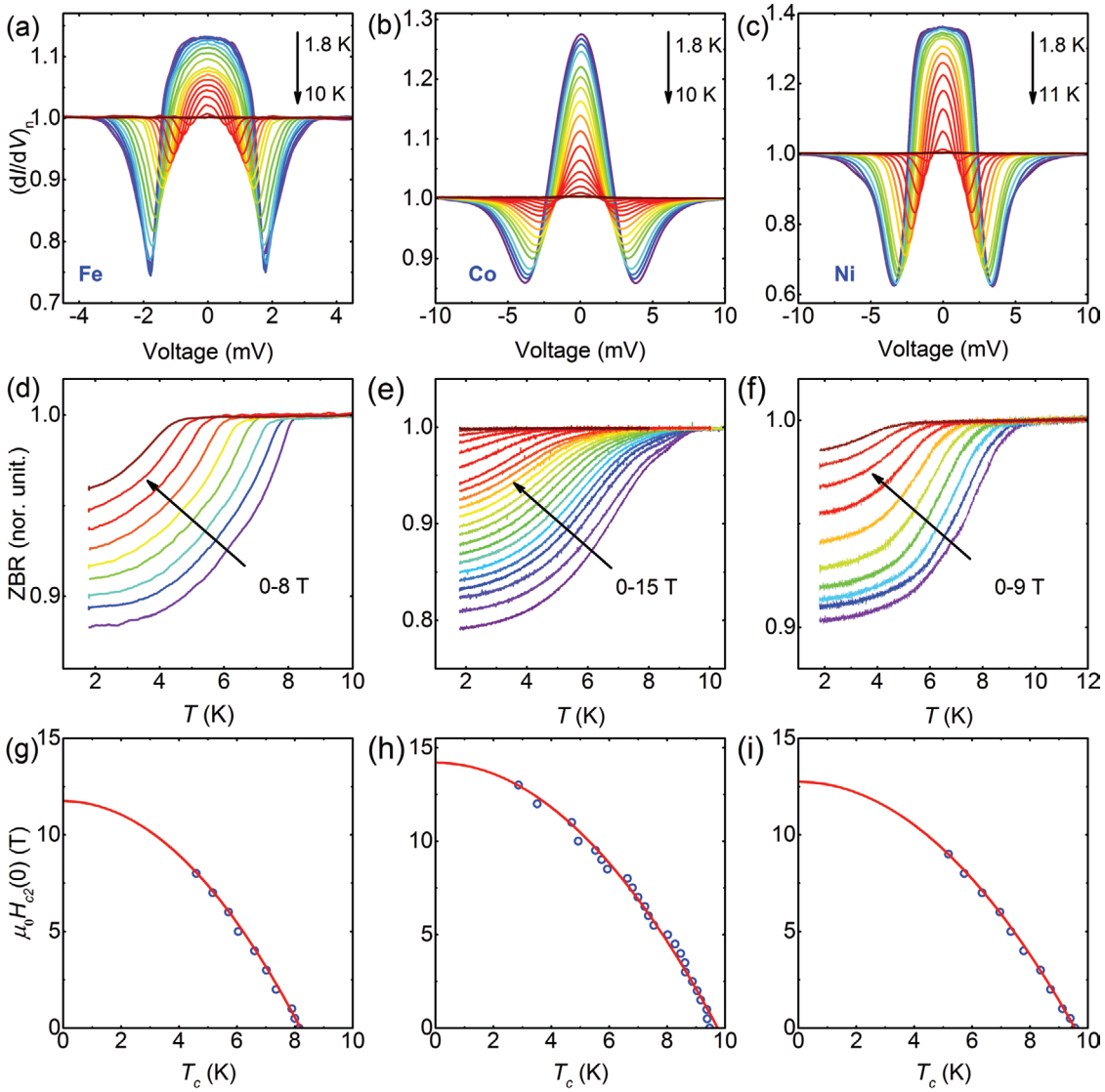

Figure 3. Temperature and magnetic field evolution of the induced superconductivity. a–c) Temperature dependence of normalized d*I*/d*V* spectra at point contacts on WC coated by magnetic Fe, Co, and Ni thin films without an external magnetic field. The temperature ranges from 1.8 to 10 K. d–f) Temperature dependence of the ZBR under several magnetic fields. g–i) The $\mu_0 H_{c2}$–T_c phase diagram extracted from (d)–(f) and fits to the data using the expression $\mu_0 H_{c2}(T) = \mu_0 H_{c2}(0)[1 - (T/T_c)^2]$.

no superconducting signals could be detected down to 1.8 K. **Figure 4**a shows a statistic chart of T_c versus film materials, in which no obvious dependence of maximum T_c value on the used film materials can be distinguished. Most impressively, there is no direct relationship between T_c and the magnetism of the materials. For the sake of further understanding, $\mu_0 H_{c2}(0)$ versus T_c is summarized in Figure 4b, which is obtained by extrapolating $\mu_0 H_{c2}(T)$ curve to zero temperature. A universal trend can be seen clearly, showing a positive correlation between $\mu_0 H_{c2}(0)$ and T_c. It is well known that, for a very thin film of conventional singlet superconductors, the superconductivity will be suppressed or even be killed by the adjacent ferromagnetic films.[37–39] In contrast to these conventional cases, the well compatibility between ferromagnetism and the interfacial superconductivity suggests the possible occurrence of unconventional superconducting states. This could be understood by two aspects: i) the deposited metals work as sources of charge transfer to the surface of WC or ii) the induced superconductivity has a triplet pairing component insensitive to ferromagnetism. The exact mechanism requires further theoretical and experimental research.

In summary, we have realized interfacial superconductivity up to 11.5 K on the surfaces of WC single crystals by coating normal metal thin films, including both nonmagnetic and ferromagnetic films. The coexistence of superconductivity and ferromagnetism is of particular interest not only for potential applications but also for the research of fundamental physics such as searching for unconventional superconductors and Majorana fermions. WC is a topological semimetal with both super hardness and high chemical stability. Using metal deposition instead of hard point contact to realize superconductivity on WC could further exclude the tip pressure or confinement

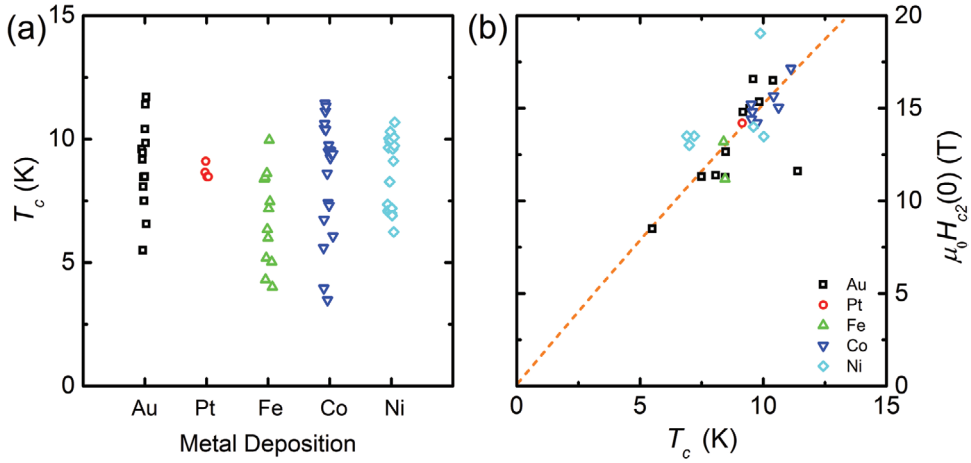

Figure 4. Critical temperatures and upper critical fields. a) Critical temperatures of the interfacial superconductivity realized on WC with diverse metal deposition. T_c is determined by the onset temperature of superconducting transition from the ZBR curves. b) Critical temperatures and upper critical fields ($\mu_0 H_{c2}(0)$) of the interfacial superconductivity realized on WC with diverse metal deposition. $\mu_0 H_{c2}(0)$ is determined by empirical formula $\mu_0 H_{c2}(T) = \mu_0 H_{c2}(0)[1 - (T/T_c)^2]$ from the magnetic field dependent ZBR. The orange dashed line is a guide to the eye.

effect as the dominant regime of such interfacial superconductivity. Then the coupling between normal metals and WC in some form is the most important ingredient of the superconductivity observed here. More experimental and theoretical work is needed to address this issue. Nonetheless, the realization of superconductivity on the topological semimetal has potential applications in designing topological superconducting devices and provides a promising platform to explore topological superconductivity in a simple and practical way.

Experimental Section

Crystal Growth and Characterization: High-quality single crystals of WC were grown from Co-fluxes. Stoichiometric amounts of W and C with moderate Co were put into graphite crucible, heated to 1700 °C, and then cooled slowly to 1400 °C in an argon atmosphere. The residual Co-fluxes were removed by dissolving in a warm hydrochloric acid solution. The obtained single crystals were in the form of equilateral triangles with sides of 1–3 mm and thickness of 0.1–0.3 mm, and were characterized by X-ray diffraction on a PANalytical diffractometer with Cu Kα radiation at room temperature. The electrical transport and magnetic characters were measured using a Quantum Design PPMS-9T, PPMS-16T, and a MPMS-7T SQUID VSM system, respectively.

Sample Fabrication and Calibration: Metallic thin films on WC single crystals were prepared using a sputtering deposition method with Au, Pt, Fe, Co, Ni targets, respectively. Scanning electron microscopy (Hitachi SU5000) was used to study the surface morphology of the prepared films. Due to the surface of WC single crystals grown at high temperature is not a smooth surface, the film thickness was determined by testing the thickness of the metal film deposited on Si substrates at a film edge using a stylus type profilometer (KLA-Tencor Profiler) and SEM.

Point-Contact Spectroscopy: Superconductivity was measured by the soft point-contact technique. The contact is made between a small drop (about 30–50 µm in diameter) of Ag paste and the metal film coating the WC surface. The Ag electrode is connected to current and voltage leads through a thin Pt wire (18 µm in diameter) stretched over the sample. Differential dI/dV spectra are measured by the standard lock-in technique. The DC current across the point contact is generated by current source (Keithley 6221) to bias the junction voltage, which is measured by a digital nano-voltmeter (Keithley 2182). A small ac current is generated by a lock-in amplifier (NF LI5640) after a voltage-to-current conversion. The first harmonic response of the lock-in is proportional to the differential change in the voltage dV.

Supporting Information

Supporting Information is available from the Wiley Online Library or from the author.

Acknowledgements

W.L.Z., X.Y.H. and J.L. contributed equally to this work. The authors acknowledge S. H. Pan and M. Q. Xue for valuable discussion. This work was supported by the Ministry of Science and Technology of China (2017YFA0302904, 2018YFA0305602, 2016YFA0401000, 2016YFA0300604, 2015CB921303), the National Natural Science Foundation of China (11574372, 11322432, 11704403, 11874417), the Chinese Academy of Sciences (XDB07020300, XDB07020100), and the Recruitment Program for Leading Talent Team of Anhui Province (2019-16).

Conflict of Interest

The authors declare no conflict of interest.

Keywords

Andreev reflections, interfacial superconductivity, metal deposition, point-contact spectroscopy, topological semimetals

Received: December 4, 2019
Revised: February 6, 2020
Published online: February 28, 2020

[1] A. Y. Kitaev, *Ann. Phys. (Amsterdam, Neth.)* **2003**, *303*, 2.
[2] C. Nayak, S. H. Simon, A. Stern, M. Freedman, S. D. Sarma, *Rev. Mod. Phys.* **2008**, *80*, 1083.

[3] A. Stern, *Nature* **2010**, *464*, 187.
[4] X. L. Qi, S. C. Zhang, *Rev. Mod. Phys.* **2011**, *83*, 1057.
[5] L. Fu, C. L. Kane, *Phys. Rev. Lett.* **2008**, *100*, 096407.
[6] U. Khanna, A. Kundu, S. Pradhan, S. Rao, *Phys. Rev. B* **2014**, *90*, 195430.
[7] P. Zareapour, A. Hayat, S. Y. F. Zhao, M. Kreshchuk, A. Jain, D. C. Kwok, N. Lee, S.-W. Cheong, Z. J. Xu, A. Yang, G. D. Gu, S. Jia, R. J. Cava, K. S. Burch, *Nat. Commun.* **2012**, *3*, 1056.
[8] H. Yang, Y. Y. Li, T. T. Liu, H. Y. Xue, D. D. Guan, S. Y. Wang, H. Zheng, C. H. Liu, L. Fu, J. F. Jia, *Adv. Mater.* **2019**, *31*, 1905582.
[9] A. P. Mackenzie, Y. Maeno, *Rev. Mod. Phys.* **2003**, *75*, 657.
[10] F. Wilczek, *Nat. Phys.* **2009**, *5*, 614.
[11] Y. S. Hor, A. J. Williams, J. G. Checkelsky, P. Roushan, J. Seo, Q. Xu, H. W. Zandbergen, A. Yazdani, N. P. Ong, R. J. Cava, *Phys. Rev. Lett.* **2010**, *104*, 057001.
[12] F. Fei, X. Y. Bo, P. D. Wang, J. H. Ying, J. Li, K. Chen, Q. Dai, B. Chen, Z. Sun, M. H. Zhang, F. M. Qu, Y. Zhang, Q. H. Wang, X. F. Wang, L. Cao, H. J. Bu, F. Q. Song, X. G. Wan, B. G. Wang, *Adv. Mater.* **2018**, *30*, 1801556.
[13] L. A. Wray, S.-Y. Xu, Y. Xia, Y. San Hor, D. Qian, A. V. Fedorov, H. Lin, A. Bansil, R. J. Cava, M. Z. Hasan, *Nat. Phys.* **2010**, *6*, 855.
[14] S. Sasaki, M. Kriener, K. Segawa, K. Yada, Y. Tanaka, M. Sato, Y. Ando, *Phys. Rev. Lett.* **2011**, *107*, 217001.
[15] T. H. Hsieh, L. Fu, *Phys. Rev. Lett.* **2012**, *108*, 107005.
[16] M. Kriener, K. Segawa, Z. Ren, S. Sasaki, Y. Ando, *Phys. Rev. Lett.* **2011**, *106*, 127004.
[17] M. Sato, Y. Ando, *Rep. Prog. Phys.* **2017**, *80*, 076501.
[18] M.-X. Wang, C. Liu, J.-P. Xu, F. Yang, L. Miao, M.-Y. Yao, C. L. Gao, C. Y. Shen, X. C. Ma, X. Chen, Z. A. Xu, Y. Liu, S. C. Zhang, D. Q, J. F. Jia, Q. K. Xue, *Science* **2012**, *336*, 52.
[19] J.-P. Xu, M.-X. Wang, Z. L. Liu, J.-F. Ge, X. Yang, C. Liu, Z. A. Xu, D. Guan, C. L. Gao, D. Qian, Y. Liu, Q. H. Wang, F. C. Zhang, Q. K. Xue, J. F. Jia, *Phys. Rev. Lett.* **2015**, *114*, 017001.
[20] L. Aggarwal, A. Gaurav, G. S. Thakur, Z. Haque, A. K. Ganguli, G. Sheet, *Nat. Mater.* **2016**, *15*, 32.
[21] H. Wang, H. Wang, H. Liu, H. Lu, W. Yang, S. Jia, X.-J. Liu, X. Xie, J. Wei, J. Wang, *Nat. Mater.* **2016**, *15*, 38.
[22] L. Aggarwal, S. Gayen, S. Das, R. Kumar, V. Süß, C. Felser, C. Shekhar, G. Sheet, *Nat. Commun.* **2017**, *8*, 13974.
[23] H. Wang, H. Wang, Y. Chen, J. Luo, Z. Yuan, J. Liu, Y. Wang, S. Jia, X.-J. Liu, J. Wei, J. Wang, *Sci. Bull.* **2017**, *62*, 425.
[24] X. Y. Hou, Z. Wang, Y. D. Gu, J. B. He, D. Chen, W. L. Zhu, M. D. Zhang, F. Zhang, Y. F. Xu, S. Zhang, H. X. Yang, Z. A Ren, H. M. Weng, N. Hao, W. G. Lv, J. P. Hu, G. F. Chen, L. Shan, *Phys. Rev. B* **2019**, *100*, 235109.
[25] D. Daghero, R. S. Gonnelli, *Supercond. Sci. Technol.* **2010**, *23*, 043001.
[26] J. B. He, D. Chen, W. L. Zhu, S. Zhang, L. X. Zhao, Z. A. Ren, G. F. Chen, *Phys. Rev. B* **2017**, *95*, 195165.
[27] G. E. Blonder, M. Tinkham, T. M. Klapwijk, *Phys. Rev. B* **1982**, *25*, 4515.
[28] R. C. Dynes, J. P. Garno, G. B. Hertel, T. P. Orlando, *Phys. Rev. Lett.* **1984**, *53*, 2437.
[29] A. Plecenik, M. Grajcar, Š. Beňačka, P. Seidel, *Phys. Rev. B* **1994**, *49*, 10016.
[30] Y. Tanaka, S. Kashiwaya, *Phys. Rev. Lett.* **1995**, *74*, 3451.
[31] G. Deutscher, *Rev. Mod. Phys.* **2005**, *77*, 109.
[32] G. Sheet, S. Mukhopadhyay, P. Raychaudhuri, *Phys. Rev. B* **2004**, *69*, 134507.
[33] N. Reyren, S. Thiel, A. D. Caviglia, L. Fitting Kourkoutis, G. Hammerl, C. Richter, C. W. Schneider, T. Kopp, A.-S. Rüetschi, D. Jaccard, M. Gabay, D. A. Muller, J.-M. Triscone, J. Mannhart, *Science* **2007**, *317*, 1196.
[34] A. V. Suslov, A. B. Davydov, L. N. Oveshnikov, L. A. Morgun, K. I. Kuge, V. S. Zakhvalinskii, E. A. Pilyuk, A. V. Kochura, A. P. Kuzmenko, V. M. Pudalov, B. A. Aronzon, *Phys. Rev. B* **2019**, *99*, 094512.
[35] J.-G. Cheng, personal communication.
[36] E. Tang, L. Fu, *Nat. Phys.* **2014**, *10*, 964.
[37] O. Bourgeois, R. C. Dynes, *Phys. Rev. B* **2002**, *65*, 144503.
[38] A. S. Sidorenko, V. I. Zdravkov, A. A. Prepelitsa, C. Helbig, Y. Luo, S. Gsell, M. Schreck, S. Klimm, S. Horn, L. R. Tagirov, R. Tidecks, *Ann. Phys.* **2003**, *12*, 37.
[39] X. X. Gong, H. X. Zhou, P. C. Xu, D. Yue, K. Zhu, X. F. Jin, H. Tian, G. J. Zhao, T. Y. Chen, *Chin. Phys. Lett.* **2015**, *32*, 067402.

